Electromagnetic Energy Coupling Path and Protection Method of UAV Datalink against Broad-Spectrum High-Power Microwave Radiation

Yuming WANG, Liyun MA, Yazhou CHEN

National Key Laboratory on Electromagnetic Environment Effects, Army Engineering University, Heping West Road 97, Shijiazhuang 050003, China

ymking2006@163.com, 271425024@qq.com, chen_yazhou@sina.com

Submitted September 6, 2021 / Accepted March 21, 2022

Abstract. *To verify the adaptability of unmanned aerial vehicle (UAV) datalinks to the electromagnetic environment comprising broad-spectrum high-power microwave radiation, strong electromagnetic pulse (EMP) tests were conducted using ultra wideband (UWB) radiation source at different radiation field strengths and repetition frequencies. For UAV datalinks, interference, disturbance, degradation and other effects were found in the tests. The electromagnetic energy coupling path of the broad-spectrum high-power microwave radiation was determined by adjusting the test status of UAV datalink as well as by protecting its key parts. The radio frequency front end, power cable and terminal interfaces on the housing surface were found to be weak electromagnetic links. The methods of the protection of radio frequency front end and power cable against strong EMPs were proposed. In addition, protection effects obtained by using different protection modules of radio frequency front end as well as by applying power spike pulse suppressors were compared and validated.*

Keywords

UAV datalink, EMP, UWB, electromagnetic environment effects, electromagnetic protection

1. Introduction

Unmanned aerial vehicles (UAVs) are high-quality combat force that is especially advantageous for tedious and dangerous task applications as well as for operations in complex environments. A UAV exchanges information with a ground control station (GCS) via the datalink. The GCS sends control commands to the UAV using uplink and then the UAV sends its own state parameters and collected task information back to the GCS using downlink. Datalink is therefore the key device for the transmission of information by UAV. The datalink interference will cause blockage of the connection, failure of the execution of task instructions and data return error. In addition, excessive coupling of electromagnetic energy can burn the radio frequency front end and power supply, which can cause fatal accidents [1–3].

Broad-spectrum high-power microwave radiation is powerful electromagnetic pulse (EMP) weapon. These electromagnetic pulses are characterized by extremely fast rising edges, ultra wide spectral bands and ultrahigh radiation field strengths. The combination of these three factors enables wide range of attacks to be made on the front- and back-doors of UAV electronic information system. Multiple studies have revealed that UAV datalink is easily interfered by strong EMPs [4] ,[5]. The survival and combat capability of UAV is directly influenced by the possibility to protect the UAV datalink against strong EMPs and to maintain a normal communication link.

2. Broad-Spectrum High-Power Microwave Radiation Tests

2.1 Broad-Spectrum High-Power Microwave Radiation Source and Radiation Field

A gigawatt (GW) ultra wideband (UWB) EMP generation system was used as the source of broad-spectrum high-power microwave radiation. This source consisted of three parts, namely UWB parabolic reflector antenna, peaking-chopping high-power ultrabroad-spectrum subnanosecond pulse generator, and Tesla primary pulsed power source. The schematic diagram of its composition and working principles are shown in Fig. 1.

This UWB radiation source could not only generate single EMPs, but also UWB EMP trains at the repetition frequency of 1, 2 and 5 Hz. UWB EMP signal is a wideband ultra-short pulse of basically Gaussian form. In this study, the emission of the radiation source was Gaussian even pulse composed of two Gaussian pulses with equal amplitudes, opposite polarities and a certain time interval.

DOI: 10.13164/re.2022.0201

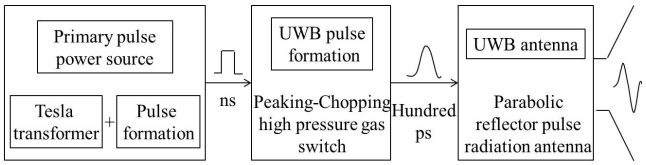

Fig. 1. Composition and principle of the UWB radiation source.

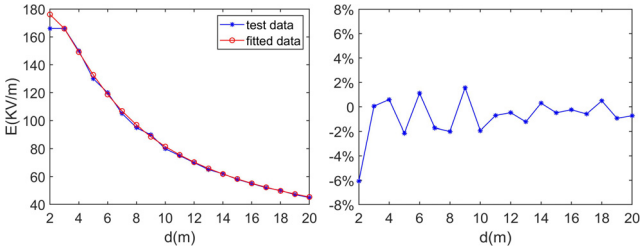

(a) Test data and fitted data. (b) Relative errors.

Fig. 2. Relation between central radiation field strength and distance of UWB radiation source.

The radiation field of UWB radiation source is tested by the calibration equipment, and the test data is shown in Fig. 2(a). The strength of the central radiation field (E, kV/m) was inversely proportional to the distance (d, m), and the relation between these two quantities is expressed as follows:

$$E = \frac{1020}{d + 2.5}\left(1 - \mathrm{e}^{-0.75d}\right). \tag{1}$$

E is the peak-to-peak value of Gaussian even pulse radiation field strength. The relative errors between (1) and the test data is shown in Fig. 2(b). Moreover, the radiation field strength had a minimum critical value. At large enough distances the radiation field is submerged in the clutter. Therefore, the conformity of the waveform of radiation field to the form of Gaussian even pulse should be monitored.

2.2 Configuration of Broad-Spectrum High-Power Microwave Test

The tested UAV datalink is shown in Fig. 3. Although the internal circuit of the datalink was shielded with a metal shell, many connection ports were exposed outside concentrated on one side of the shielding shell. Moreover, the interconnection cables, which included signal line, power line and control line, were mostly unshielded. If a stabilized voltage supply is used in the strong EMP test, the EMP will very probably be coupled with the power cable, thus triggering the voltage pulses to damage the voltage supply. This phenomenon was confirmed in at least three tests on three datalinks. Given this, a storage battery power supply was used in our tests.

The airborne end and ground end of the datalink could be tested separately. According to the task settings, the airborne end is susceptible to harsh electromagnetic environment after the takeoff of the UAV, while the ground

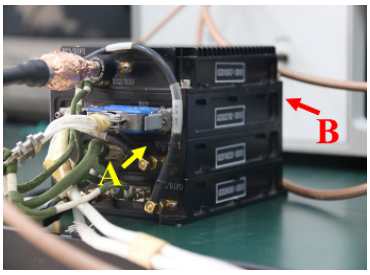

Fig. 3. Airborne end of the tested UAV datalink.

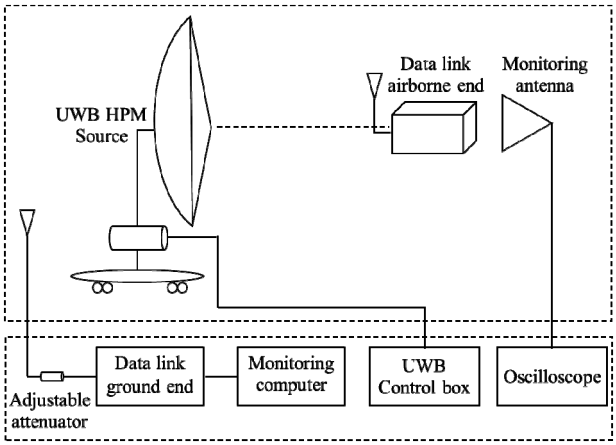

Fig. 4. UWB irradiation test system and configuration.

end remains mostly in the controllable electromagnetic environment. Therefore, only the airborne end of the datalink was tested. The test was carried out in an open field to simulate the real UAV flight state and apply the radiation field strength from a wider range. A receiving antenna was set to monitor the waveform of the radiation field. An adjustable attenuator was used to simulate the UAV flight state in the air according to reference [3]. An adjustable attenuator is needed because of the dynamic change of the jamming-to-signal ratio received by datalink, due to the change of the flight distance, altitude and other flight parameters. The test system and configuration is shown in Fig. 4.

3. Electromagnetic Environmental Effect and Electromagnetic Energy Coupling Path

3.1 Electromagnetic Environmental Effect Levels

According to the impact of broad-spectrum high-power microwave radiation on datalink functionality, four levels of the electromagnetic environmental effect are distinguished, namely: interference, disturbance, degradation and damage.

Interference is defined as a short-term loss of the datalink lock that can be restored spontaneously. “Loss of

lock" and "locking" of the datalink are directly inferred by the monitoring indicator at the ground end. "Loss of lock" means that the airborne end of the datalink cannot interact with the ground end and no communication link can be established. "Locking" indicates that the interconnection link is enabled and the reception/transmission function can be normally completed.

Disturbance means that the datalink cannot be self-restored after loss of lock and the link can be reestablished only when a control command is sent by the ground end.

At degradation the datalink subjected to loss of lock cannot be restored even if a control command is sent by the ground end. Instead, it can be restored only by re-electrifying the airborne end of the datalink.

Damage refers to any hardware damage of the datalink.

3.2 Electromagnetic Energy Coupling Path

The electromagnetic energy coupling path of UAV datalink for broad-spectrum high-power microwave radiation was verified using iterative tests. These tests were carried out at different values of the radiation field strength and repetition frequency of the UWB radiation source. In addition, the effects of a number of protective measures were studied. The test results are listed in Tab. 1.

The low critical value of the field strength of the UWB radiation source was 48.6 kV/m. The monitored waveform of radiation field was not ideal at large distances. When the airborne end of the datalink was placed in the irradiated zone and the surface A with collectively exposed ports (Fig. 1) faced the incoming wave, the datalink crashed after ten repeated tests no matter whether a single triggered pulse or the pulses at repetition frequency

Strength (kV/m)	Test No.	Test status	Repetition frequency			
			single trigger	1 Hz	2 Hz	5 Hz
48.6	1	Surface A faced the incoming wave.	Degradation (10/10).	Degradation (10/10).	Degradation (10/10).	Degradation (10/10).
	2	Surface B faced the incoming wave.	Normal (7/10); Interference (3/10).	Interference (10/10).	Interference (10/10).	Interference (10/10).
58.8	3	Surface B faced the incoming wave.	Normal (2/10); Interference (7/10); Degradation (1/10).	Interference (10/10).	Disturbance (10/10).	Interference (5/10); Degradation (5/10).
71.0	4	Surface A faced the incoming wave.	Degradation (10/10).	Degradation (10/10).	Degradation (10/10).	Degradation (10/10).
	5	Surface B faced the incoming wave.	Interference (5/10); Degradation (5/10).	Degradation (10/10).	Degradation (10/10).	Degradation (10/10).
96.4	6	Surface B faced the incoming wave.	Degradation (10/10).	Degradation (10/10).	Degradation (10/10).	Degradation (10/10).
	7	The airborne end and storage battery were wrapped with shielding cloth. Only the power cable between them was exposed to microwave radiation.	Interference (10/10).	Interference (10/10).	Interference (10/10).	Interference (10/10).
	8	The antenna and the cable connecting antenna with the radio frequency front end were exposed to EMPs. The rest were all placed in shielded box.	Normal (6/10); Interference (4/10).	Interference (10/10).	Interference (10/10).	Interference (10/10).
	9	Only the antenna was exposed to EMPs. The rest were all placed in shielded box.	Normal (10/10).	Normal (8/10); Interference (2/10).	Interference (10/10).	Interference (10/10).
129.0	10	Surface B faced the incoming wave.	Degradation (10/10).	Degradation (10/10).	Degradation (10/10).	Degradation (10/10).
151.6	11	Surface B faced the incoming wave.	Degradation (10/10).	Degradation (10/10).	Degradation (10/10).	Degradation (10/10).
	12	Only the antenna was exposed to EMPs. The rest were all placed in shielded box.	Normal (6/10); Interference (4/10).	Interference (10/10).	Interference (10/10).	Interference (10/10).
165.9	13	Surface B faced the incoming wave.	Degradation (10/10).	Degradation (10/10).	Degradation (10/10).	Degradation (10/10).
	14	Only the antenna was exposed to EMPs. The rest were all placed in shielded box.	Interference (10/10).	Interference (10/10).	Interference (10/10).	Interference (10/10).

Tab. 1. Test results.

of 1, 2 and 5 Hz were emitted by the UWB radiation source. The datalink could restore the operation only after being re-electrified. The data recorded in the test were the level of effect and degradation probability (10/10).

The data of the test obtained at the same value of the radiation field strength, but with the surface A turned away from the incoming wave and the surface B toward it, are presented in test 2 in Tab. 1. At the single-trigger mode of the UWB radiation source the datalink showed normal communication for seven times and interference for three times in the series of ten tests. When the repetition frequency of the UWB radiation source was 1 Hz the datalink was interfered in all the ten tests. At the repetition frequency of 2 Hz it was disturbed all the times. As the repetition frequency was 5 Hz, the datalink was interfered in five tests and degraded in the other five tests. Despite the repetition frequency, the observed effects were smaller as compared to the situation with the surface A facing the incoming wave. It is preliminarily concluded therefore that the cable and connection ports are important paths for electromagnetic energy coupling.

The data of the test obtained in the same configuration of the airborne end of the datalink but at the radiation field strength increased to 58.8 kV/m, are displayed in test 3 in Tab. 1. Aggravation of the negative effects with the increase in the radiation field strength was observed. At the same radiation field strength the airborne end of the datalink was susceptible to the repetition frequency of the UWB radiation source. To be more specific, the higher was the repetition frequency, the stronger were the observed effects.

The surfaces A and B at the airborne end of the datalink were tested separately after the radiation field strength was increased to 71.0 kV/m, and the results are displayed in test 4 and test 5 in Tab. 1. While verifying the electromagnetic susceptibility of cable and connection port, this group of data further indicated the significant influence of the radiation field strength on the datalink system in comparison with the data of test 2, test 3 and test 5 under the same test status, as well as test 6 in which the radiation field strength was increased to 96.4 kV/m. Meanwhile, the threshold of radiation field strength at which the tested datalink experienced performance degradation under the wide-spectrum high-power microwave was basically explored.

In the following test, the key parts of the datalink were safeguarded and the weak electromagnetic links were created in an effort to reveal the electromagnetic energy coupling paths. The interconnection cables at the airborne end of the datalink included power line, signal line and control line. In the test, the surface B faced the incoming wave and the airborne end of the tested datalink and storage battery, together with the connection port and exposed aperture were wrapped with shielding cloth. Only the power cable between them was exposed to microwave radiation. The test was carried out at the radiation field strength of 96.4 kV/m. The test results are shown in test 7 in Tab. 1.

It was demonstrated by comparison with early stage test data that the exposed signal line and connection port are coupled with strong EMP energy. The electromagnetic energy coupling can be blocked to a certain extent by shielding. However, the interference was observed in all the cases. This indicates that the exposed power line and radio frequency front end are the interference energy coupling paths for the datalink, and that the shielding cloth may have insufficient shielding efficiency.

Therefore, the airborne end of the datalink, storage battery and the power line between them were placed together in a metallic shielding box. Only the transmitting/receiving antenna at the airborne end was exposed to EMPs. It was connected to the internal radio frequency front end at the airborne end via a segment of cable. The test was then implemented at the constant radiation field strength of 96.4 kV/m. The test data are shown in test 8 in Tab. 1.

Comparison between the results of test 7 and test 8 illustrates that the power cable is a coupling path leading to the electromagnetic interference of the datalink. In these both tests power line ports were shielded. If all the ports were exposed, the effects triggered by the electromagnetic energy coupled with the power supply system would be aggravated. Test 8 also indicates that the radio frequency front end is an important path for the electromagnetic interference at the airborne end of the UAV datalink.

To tackle the interference phenomenon detected in test 8, the cable connecting the transmitting/receiving antenna with the radio frequency front end was placed in the shielding box (Fig. 5). Due to the variety of energy coupling paths under strong electromagnetic pulse, it is difficult to accurately measure the protection effectiveness of a single protection method. They are comprehensive protection effects. The shielding efficiency of the shielding box we use is about 80 dBs. The purpose of using it is to assist in verifying the electromagnetic effect that can be achieved only through the RF front-end.

The radiation field strength was maintained at 96.4 kV/m. The results of this test can be seen in test 9 in Tab. 1. In this case, the transmitting/receiving antenna was the only coupling path with electromagnetic interference energy. It is illustrated by comparison of the results obtained in test 8 and test 9 that the protection of radio frequency front end should be considered as the highest priority. If the antenna is connected to the receiver via a cable, this cable must be also protected.

Subsequently, in order to verify the ability of the broad-spectrum high-power microwave radiation to damage the UAV datalink in the actual configuration, the air-borne end of the datalink was turned to the initial exposed state, while the surface B was turned to face the incoming wave. The radiation field strength was increased to 129.0 kV/m,

Fig. 5. Configuration of test 9 in Tab. 1.

151.6 kV/m and 165.9 kV/m. Respective test data are shown in test 10, test 11 and test 13 in Tab. 1. These results demonstrate that the datalink did not experience any hardware damage even at the maximum stable radiation field strength (165.9 kV/m) produced by the UWB radiation source.

In order to verify the electromagnetic effect only due to the electromagnetic energy coupled with the antenna at the radio frequency front end, we conducted the test at the radiation field strength of 151.6 kV/m and 165.9 kV/m in the configuration shown in Fig. 5 (test 12 and test 14 in Tab. 1). Comparing the data of the test 9, test 12 and test 14 obtained in the same configuration, we found out that strong EMP energy coupled at the radio frequency front end of the datalink leads to unavoidable datalink interference. Therefore, strong EMP can be effectively suppressed only by reinforcement measures at the radio frequency front end.

4. Method of UAV Datalink Protection against Strong Electromagnetic Fields

4.1 Electromagnetic Protection at the Radio Frequency Front End of Datalink

The radio frequency front end is the focus of the electromagnetic protection of datalink. The integrated anti-interference and anti-damage design of the radio frequency front end, which takes into consideration the electromagnetic protection requirements and index distribution, is a perfect solution. However, in order to compare the electromagnetic protection effects on many frequency equipment, an electromagnetic protection module was installed outside the radio frequency front end. Such method of electromagnetic protection is commonly used at present [6–8].

Four protective modules were designed to conform to the working frequency band of the radio frequency front end of the datalink. All modules, which could realize two-way transmission, were directly placed at the rear end of the transmitting/receiving antenna. The main parameters of these modules are presented in Tab. 2.

To observe and compare the protective properties of such modules, the main body of the airborne end of the datalink was first removed. The protection effect was directly observed with the transmitting/receiving antenna. The waveforms of the broad-spectrum high-power microwave radiation received by the tested datalink antenna in the no-load state were detected as shown in Fig. 6(a). The waveform on the right is one of the monitoring signals received by the antenna adapted to the UWB radiation source. On the left, the waveform of the signal received by the transmitting/receiving antenna of the datalink is presented. The peak induced voltage was about 2,009 V and the duration of the main pulse peak was approximately equal to that of the UWB radiation source.

It is not clear whether the voltage induced by the broad-spectrum high-power microwave radiation, having passed the protective modules, falls within the tolerance range of the receiver at the airborne end. Therefore, the protective module 1 with the maximum pulse power capacity was used for the test. This protective module was designed based on the design of the integrated protective modules against nuclear and lightning EMPs. The insertion loss of the protective module we used was less than 0.45 dB in the working frequency range of the tested datalink. The transmitting/receiving antenna of the datalink was connected to the protective module 1 and the waveforms of the signals measured in the no-load state at the rear end are shown on the left in Fig. 6(b).

It can be seen that the peak value of the leakage signal reached about 812 V indicating insufficient protective effect. In the test conducted using two protective modules 1 in tandem connection instead of a single one, the measured waveforms were basically identical to those shown in Fig. 6(b). This manifests that the power capacity of a single protective module is actually sufficient and that the inhibiting effect is not much different from the one achieved by using two modules. The reason for the insufficient protective effect is rather low response speed. While the duration of the rising edge of the UWB radiation was 1 ns, the amplitude limiting response speed of protective module 1 was 2 ns, which led to high leakage and hence insufficient protective capability.

Adjusting the combinations of protective modules, the module 1 was tested in tandem connection with the module 3

Module No.	Insertion Loss	Response Time	CW Power Handling	Peak Power Handling
1	< 0.45 dB	< 2 ns	50 dBm (100 W)	60 dBm (1000 W)
2	< 0.65 dB	< 1 ns	33 dBm (2 W)	43 dBm (20 W)
3	< 0.70 dB	< 1 ns	40 dBm (10 W)	50 dBm (100 W)
4	< 0.85 dB	< 1 ns	53 dBm (200 W)	56 dBm (320 W)

Tab. 2. Protective modules.

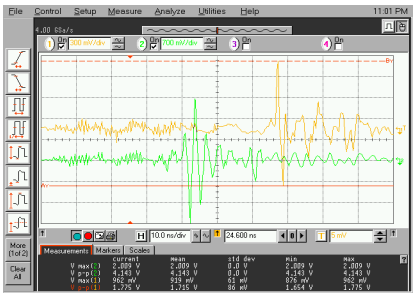

(a)

(b)

Fig. 6. Waveforms received by the antenna: (a) UWB signal waveforms received by the antenna at the airborne end of datalink in the no-load state. (b) Test waveforms of the signals received by antenna connected to protective module 1.

(a)

(b)

Fig. 7. Protective modules and waveforms received by the antenna: (a) Protective module 1 in tandem connection with protective module 3. (b) Test waveforms of the signals received by antenna using protective module 1 in tandem connection with protective module 3.

as shown in Fig. 7(a). The initial goals were first to prevent the protective modules from burning, and then to raise the response speed to the highest possible extent. The protective effect of this module combination is shown in Fig. 7(b). The energy of the pulse was suppressed and the peak value of induced voltage was about 306 V. Therefore, the feasibility of the protection strategy using such module combination is proved.

(a)

(b)

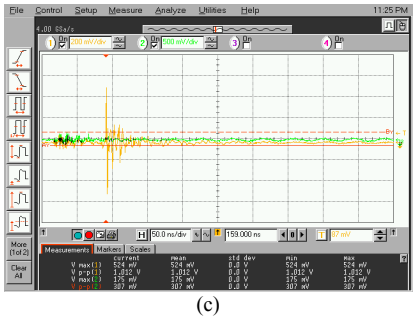

(c)

Fig. 8. Waveforms received by the antenna connected to protective modules: (a) Test waveforms of the signals received by the antenna connected to protective module 2. (b) Test waveforms of the signals received by the antenna connected to protective module 3. (c) Test waveforms of the signals received by the antenna connected to protective module 4.

According to the results of test 13 presented in Tab. 1, no hardware damage was caused to the radio frequency front end at the airborne end of the datalink under the maximum radiation field strength of the UWB radiation. Therefore, a comparative test was carried out by directly connecting the protective modules 2, 3 and 4 to the transmitting/receiving antenna. The waveforms received by antenna connected to different protective modules in the no-load state are shown in Fig. 8(a), (b) and (c).

The response speeds of all three protective modules were lower than 1 ns. Therefore, the modules could timely respond to the rising edge of the UWB radiation. Their insertion losses were smaller than 1 dB, showing minor influence on the receiving channel of the datalink. The three modules differed by the power capacity and the corresponding initial limiting voltage of the device at each level, power capacity of single-level device, and impedance

Strength (kV/m)	Test No.	Test status	Repetition frequency			
			Single triggered	1 Hz	2 Hz	5 Hz
151.6	15	Antenna connecting protective module 1 was exposed to EMPs. The rest were all placed in shielded box.	Normal (10/10)	Normal (10/10)	Normal (10/10)	Normal (10/10)
	16	Antenna connecting protective module 2 was exposed to EMPs. The rest were all placed in shielded box.	Normal (10/10)	Normal (10/10)	Normal (10/10)	Normal (10/10)
	17	Antenna connecting protective module 3 was exposed to EMPs. The rest were all placed in shielded box.	Normal (10/10)	Normal (10/10)	Normal (10/10)	Normal (10/10)

Tab. 3. Test results.

matching at each level. The design of module 2 was consistent with protective module 4, and both modules differed from protective module 3.

In the no-load state, the peak value of the induced voltage was about 242 V after connection of the transmitting/receiving antenna at the airborne end of the datalink to the protective module 2, 205 V after connection to the protective module 3, and 524 V after connection to the protective module 4. It was preliminarily estimated that the airborne end of the datalink could tolerate the residual transient voltage. Therefore, the tolerance test of the airborne end of datalink was carried out by connecting protective modules to the radio frequency front end. The results of this test are listed in Tab. 3.

Table 3 shows the test results after protection, and the data link works normally, of course, when other backdoor coupling is well suppressed. We also draw the following conclusions.

(1) The test data obtained for connections of single protective modules 2, 3 and 4 were compared. The results showed that it was unnecessary to try for the highest power capacity as long as the protective capability was sufficient. The higher power capacity meant more protective devices, more complicated design, higher insertion losses, higher leakage and greater impact on the regular transmission of working signal. However, protective modules with sufficient power capacity must be installed in wartime to prevent them from being destroyed by high-power weapons.

(2) Under normal circumstances, the higher power capacity implies higher leakage voltage. However, the effect of protective module 3 with higher power capacity was superior to that of protective module 2, indicating better single-level device performance, matching degree and design of module 3 as compared to those of module 2.

(3) The inhibiting effect reached by the protective module 3 in tandem connection with the protective module 1 was poorer than the one reached by the protective module 3 alone. This is because the protective module 1 started first to limit the amplitude of the broad-spectrum high-power microwave signal received by the transmitting/receiving antenna. However, EMP energy partially leaked due to the insufficient response speed of the module 1, and this part of energy was inhibited by the protective module 3. At this, the high-power coarse-tuning protective device of the protective module 3 did not start due to the attenuated pulse strength, and only fine-tuning protective devices at subsequent levels started. Therefore, the protective effect was not as good as that of the overall construction. Nevertheless, this combined design provided a good solution to improve the power capacity of protective modules and increase the amplitude limiting response speed at the same time. When the protective module 1 was in tandem connection with the protective module 3, the through-current capability of lightning EMP and the response speed of about 1 ns were realized.

(4) When the radiation field strength reached 165.9 kV/m the interference took place in both single trigger mode and at all the repetition frequencies of the UWB radiation independently on the protective modules used. This suggests that at high enough values of the radiation field strength of broad-spectrum high-power microwave radiation the frequency equipment is affected anyways.

4.2 Electromagnetic Protection of Power Supply System

Due to the unreliability of the power supply system, the hardware of the power supply device or the internal power supply network of the tested datalink were damaged in nuclear EMP test and electrostatic EMP test. The reliability of the power supply is the basis for the conduction of the broad-spectrum high-power microwave radiation tests. Therefore, the configuration of the electromagnetic protection of power supply system will be highlighted.

The original UAV datalink used twisted-pair power cable. The airborne end of the datalink and storage battery were separately placed in the shielding box to test the interference caused by the power cable. When the radio frequency front end was equipped with protective modules and the radiation field strength was reduced to 20.8 kV/m, respective test data are shown in test 18 in Tab. 4. It can be seen that the airborne end of the datalink was interfered despite very low strength of the radiation field produced by the UWB radiation system. This proves that the broad-spectrum high-power microwave radiation is harmful in a wide frequency range, including the working L-band of the tested datalink and the low-frequency band of cable coupling.

Strength (kV/m)	Test No.	Test status	Repetition frequency			
			Single triggered	1 Hz	2 Hz	5 Hz
20.8	18	The twisted-pair power cable was exposed to EMPs.	Normal (5/10); Interference (5/10).	Interference (10/10).	Interference (10/10).	Interference (10/10).
151.6	19	The high-performance shielded cable was exposed to EMPs.	Normal (10/10).	Normal (10/10).	Interference (10/10).	Interference (10/10).

Tab. 4. Test results.

The test data obtained using high-performance shielded cable are shown in test 19 in Table 4. The datalink functioned normally at the radiation field strength below 151.6 kV/m. It was interfered, however, when the radiation field strength reached 151.6 kV/m, at the repetition frequency of 2 and 5 Hz.

To further study the interference suppression, the original twisted-pair cable was used for power supply. As shown in Fig. 9, the positive and negative electrodes were connected to the power spike pulse suppressor at the proximal end of the airborne end of the datalink. Of course, this configuration is to verify the energy coupling path and the protection effect. In the actual application of UAV, the energy suppression chip is directly integrated in the power supply. Normal operation of the datalink was observed at the radiation field strength of 151.6 kV/m in the single trigger mode and at the repetition frequency of the UWB radiation source of 1, 2 and 5 Hz. Obtained results demonstrate that the field-line coupling was not the only interference caused by the power cable. Due to the short time of the rising edge and the wide band of the broad-spectrum high-power microwave radiation, spike pulse could be coupled still with the internal supply circuit of the datalink via the transit port and the shell gap. Therefore, the interference should be completely suppressed prior to connecting the power cable to the system.

The test results did not change when only the positive electrode was connected to the power spike pulse suppressor or when both the positive and negative electrodes were connected to it. This proves that the grounding system used in the test was relatively stable and that a good effect can be obtained by merely suppression of the power spike pulse on the positive electrode. However, the stable grounding system in the ground test is not necessarily applicable to real UAV datalinks. Therefore, the power spike pulse suppressor should be connected to both positive and negative electrodes.

When the power spike pulse suppressor was connected to only the negative electrode, the datalink degradation was observed at the radiation field strength of 151.6 kV/m in the single trigger mode of the operation of UWB radiation source. Strong EMPs could be seen to enter the circuit by cable line coupling, which caused voltage spikes and glitching and seriously interfered normal circuit operation.

Generally speaking, installation of the power spike pulse suppressor in parallel with the power cable can effectively prevent the strong EMP. Suppression of the spike pulse only on the ground wire cannot completely eliminate the ground potential fluctuations. Therefore, this method is not very effective. Systematic design should be applied for protection of the power supply against strong EMPs. Moreover, application of shielded cables, installation of parallel spike pulse suppressors and high-quality grounding are effective protection methods.

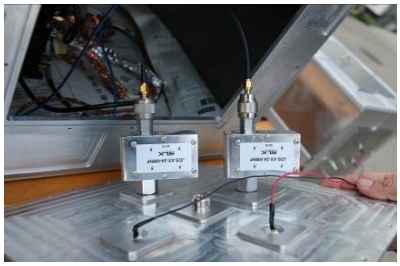

Fig. 9. Power spike pulse suppressor connected to the airborne end of datalink.

4.3 General Protection Methods

The general protection methods for UAV datalinks include shielding, filtering and grounding [9], [10]. To protect the datalink, it is necessary to use shielding shells, follow the basic principles of electromagnetic compatibility design, apply particular opening sizes and directions of connection ports, and employ the cut-off waveguide ventilation plates for ventilation and dissipation of heat. All the exposed interconnection cables including the signal line, control line and power line must be shielded. Moreover, attention should be paid to the high quality of grounding and bonding. To prevent the strong EMP interference, electromagnetic interference filters and power cable filters are mainly used in filter design. The filters should enable sufficient level of interference suppression. They should be installed in parallel and on the panel. Besides, to effectively suppress strong EMPs in the grounding system, shielding, filtering and grounding should be applied throughout in addition to following the design rules for equipment grounding. In other words, shielding shells, shielded cables, electromagnetic interference filters and power spike pulse suppressors must be well grounded.

5. Conclusion

UAV datalink is highly sensitive to the broad-spectrum high-power microwave radiation. Its coupling paths

include the radio frequency front end in the frequency range of the broad-spectrum high-power microwave radiation as well as the back-door coupling of various cables, connection ports and apertures. Protection against strong EMPs at the radio frequency front end should be given especial attention. Installation of additional suitable protective modules or implementation of integrated protection chips are the main measures. Usually, protective modules with small insertion losses and power capacities meeting application demands can be used. However, in wartime, some useful signal power can be sacrificed enabling to install protective modules with high power capacity to resist the impact of high radiation field strength. In addition, the multiplication effect can be achieved using appropriate back-door protection design. In particular, protection of the power supply network against strong EMPs can be enhanced by installing power spike pulse suppressors in parallel at the proximal end of the equipment and using high-performance shielded cables to supply power. In general, as UAVs are typically used to execute tasks in complex electromagnetic environment, reliable remote data transmission is required.

Reference [3] and [5] are also the research results of our team. Reference [3] proposed a datalink model of UAV in different flight states, with the purpose of replacing air test with ground test and dynamic test with static test. It is by using this model that the equivalent configuration for simulating UAV flight status on the ground is realized. Reference [5] is the effect analysis of UAV datalink under narrow-spectrum high-power microwave. This paper deals with the propagation coupling path and corresponding protection method of UAV datalink under ultra-wide spectrum high-power microwave. Reference [3], [5] and this paper are systematic research results. By integrating references [3], [5] and this paper, a more complete conclusion can be drawn.

References

[1] ZHANG, D. X., CHEN, Y. Z., CHENG, E. W., et al. Effects of electromagnetic interference (EMI) on information link of UAV. *Transactions of Beijing Institute of Technology*, 2019, vol. 39, no. 7, p. 756–762. (In Chinese) DOI: 10.15918/j.tbit1001-0645.2019.07.016

[2] DU, B. Z., CHEN, Y. Z., CHENG, E. W., et al. Experiment analysis of continuous wave electromagnetic irradiation effect for a certain type of UAV data link. *Journal of Microwaves*, 2018, vol. 34, no. 2, p. 86–91. (In Chinese) DOI: 10.14183/j.cnki.1005-6122.201802017

[3] ZHANG, D. X., CHENG, E. W., WAN, H. J., et al. Prediction of electromagnetic compatibility for dynamic datalink of UAV. *IEEE Transactions on Electromagnetic Compatibility*, 2019, vol. 61, no. 5, p. 1474–1482. DOI: 10.1109/TEMC.2018.2867641

[4] SAKHAROV, K. Y., SUKHOV, A. V., UGOLEV, V. L., et al. Study of UWB electromagnetic pulse impact on commercial unmanned aerial vehicle. In *2018 International Symposium on Electromagnetic Compatibility (EMC EUROPE)*. Amsterdam (Netherlands), 2018, p. 40–43. DOI: 10.1109/EMCEurope.2018.8484992

[5] ZHANG, D. X., ZHOU, X., CHENG, E. W., et al. Investigation on effects of HPM pulse on UAV's datalink. *IEEE Transactions on Electromagnetic Compatibility*, 2019, vol. 62, no. 3, p. 829–839. DOI: 10.1109/TEMC.2019.2915285

[6] HAO, R. R., ZHANG, X. D., GAO, H., et al. A novel high-altitude electromagnetic pulse (HEMP) protection circuit for RF applications. *Microelectronics Journal*, 2019, vol. 84, no. 2, p. 1–8. DOI: 10.1016/j.mejo.2018.12.005

[7] LI, Y. N., TAN, Z. L. Design and research of the fast rise time electromagnetic pulse protection module based on PIN diode. *Acta Armamentarii,* 2018, vol. 39, no. 10, p. 2066–2072. (In Chinese) DOI: 10.3969/j.issn.1000-1093.2018.10.021

[8] LI, Y. N., TAN, Z. L., PENG, C. Z., et al. Simulation and design of RF front end electromagnetic protection module based on HF communication. *Acta Electronica Sinica*, 2018, vol. 46, no. 6, p. 1421–1427. (In Chinese) DOI: 10.3969/j.issn.0372-2112.2018.06.022

[9] DU, B. Z., CHEN, Y. Z., CHENG, E. W. Strong electromagnetic pulse comprehensive protection methods research for UAV. In *The 2nd International Conference on Mechatronics Engineering and Information Technology (ICMEIT)*. Dalian (China), 2017, p. 1–4. DOI: 10.2991/icmeit-17.2017.1

[10] ZHOU, P., LV, Y. H, SONG, Y. S., et al. Discussion on transient electromagnetic pulse protection methods of aerospace system. In *The 7th Asia-Pacific Conference on Environmental Electromagnetics (CEEM)*. Hangzhou (China), 2015, p. 405–407. DOI: 10.1109/CEEM.2015.7368716

About the Authors ...

Yuming WANG was born in 1980. She received her Ph.D. degree at Mechanical Engineering College. Her interest is in the electromagnetic compatibility and electromagnetic protection.

Liyun MA was born in 1984. She received her M.D. degree at Shaanxi University of Science and Technology. Her interest is in the electromagnetic compatibility and electromagnetic protection.

Yazhou CHEN was born in 1975. He received his Ph.D. degree at Mechanical Engineering College. His interests are in the simulation of environment effects of strong electromagnetic fields, electromagnetic environment effects and protection.